

Paper Reference No: MWF09 PN-164

Spectral Angle Mapping and Linear Spectral Unmixing of the ASTER data for alteration mapping at Sarduiyeh area, SE Kerman, Iran

**Presenter: Majid H.Tangestani
Majid H.Tangestani and Mahdieh .Hosseinjani**

Dept. of Earth Sciences, Faculty of Sciences, Shiraz University, 71454 Shiraz, Iran

E-mail: tangestani@susc.ac.ir, mh.hosseinjani@gmail.com

Telephone number: 0098-7116137222

Fax number: 0098711613



Tangestani M.H, Assistant Prof in Shiraz University

Hosseinjani M, PhD student in Shiraz University

Abstract:

An area located at the Central Iranian Volcano-Sedimentary Complex is tested for mineral mapping using the ASTER data. The L1B dataset of ASTER was calibrated using the Internal Average Relative Reflection (IARR) method. Spectral Angle Mapping (SAM) and Linear Spectral Unmixing (LSU) algorithms were applied to mapping alteration minerals using the image spectra and the spectra selected from USGS library. Spectra of the image were extracted using the "spectral end-member selection" procedures, including minimum noise fraction (MNF), pixel purity index (PPI) and n-dimensional visualization.

Since the kaolinite, white mica and montmorillonite share a diagnostic absorption feature in band 6 of ASTER they were considered as one group (argillic alteration indicators) in image analyses. The spectra of alunite and pyrophyllite are characterized by a diagnostic absorption feature in band 5 and are evidences for advanced argillic alteration. Finally, chlorite, epidote and calcite, showing a common absorption feature in band 8 were selected for discriminating propylitic alteration zone.

Linear Spectral Unmixing using the image spectra obtained reasonable results and successfully discriminated pixels with highest proportions of alteration minerals, around copper deposits; while the abundance values of end-members selected from the USGS spectral library were not satisfied for output pixels. Pixels discriminated as alteration minerals generally were corresponded to the alteration zones mapped by the National Iranian Copper Company for Daralu deposit.

It is concluded that outputs obtained from the SAM and LSU algorithms were more reliable when using the ASTER image spectra in comparison to using spectra from the USGS library. Furthermore, LSU and SAM algorithms discriminated similar regions for each alteration zone when using the image spectra.

1- Introduction:

One of the main aims of geological remote sensing has been the development of methods for mineral mapping and rock type discrimination. The exploration geologist

pay more attention to hydrothermally altered rocks and clay minerals because of their potential economic importance and diagnostic spectral features as a key for their identification via remote sensing techniques.

Many commonly used spectral analysis techniques such as Spectral Angle Mapping and Linear Spectral Unmixing are based on the fact that remotely sensed imagery are sampled with numerous spectral bands at narrow bandwidths (often on the order of tens of nanometers), making it possible to construct a spectrum for each pixel in the image. The spectrum can then be compared with the spectra of known pure materials such as minerals, vegetation, and soil, and pixels which are similar to this spectrum could be distinguished. Many techniques, despite their primary design for use with hyperspectral data, can be applicable logically to multispectral data such as ASTER.

The pure materials are often referred to as endmembers. The spectra of the endmembers primarily come from three different sources including: image derived “pure pixels”, in situ spectroradiometric measurement, and laboratory based spectral libraries such as, United State Geological Survey (USGS), Johns Hopkins University (JHU) and the NASA’s Jet Propulsion Laboratory (JPL).

Spectral Angle Mapping and Linear Spectral Unmixing techniques were applied by many researchers in remote sensing studies (Kruse et al. 1993, Boardman et al 1994, Van Deer Meer 1995, 1996, 1999, 2001, Galvao et al 2001, Rowan et al 2003, 2006, Qui et al 2006, Tangestani et al 2005, 2008). These algorithms were implemented based on the comparison of a pixel spectrum with the spectra of known pure materials.

The purpose of this paper is to employ Spectral Angle Mapping (SAM) and Linear Spectral Unmixing (LSU) algorithms on the ASTER data to discriminating alteration zones in the Sarduiyeh, SE Kerman Province, Iran. Analysis focus on the spatial distribution of the main types of hydrothermally altered minerals including kaolinite, alunite and chlorite. Image and laboratory spectra of these minerals were used to perform algorithms.

2- Geological setting:

The study area ($57^{\circ} 00' - 57^{\circ} 30' E$ and $29^{\circ} 00' - 29^{\circ} 30' N$) is situated in the southern part of Central Iranian Volcano- sedimentary complex (Uromiye- Dokhtar belt), south-southeast of Kerman province (Fig. 1). This belt has a great potential for the exploration of porphyry copper mineralization.

The most impressive geological feature in this area is the Eocene sequences, consisting of andesite, andesite-basalt, basalt, rhyolite, trachyte, trachyandesite, trachybasalt and their pyroclastics. Horizons of limestones, conglomerates and sandstones are also exposed at the area. The Eocene sequence is intruded by Oligo–Miocene granodiorite, quartz-diorite, diorite, monzonite, tonalite and granite plutons. Alteration zones and copper mineralization are generally related to the hydrothermal solutions. Hydrothermal alterations occur in both the Eocene volcanics and intrusive plutons. Argillization, sericitization, propylitization and silification are the most common types of hydrothermal alterations in the area (Geological Survey of Iran 1973).

Copper occurrences are numerous, some of them being exploited in the ancient time. Mineralized veins, mostly in Eocen volcanics, are situated along the highly silicified faults. They are mineralized by chalcopyrite, pyrite, bornite and magnetite. Veins are mostly at Kuh-e- Bahr Aseman, Kuh-e-Hanza, and near the Godar Siah. Porphyry copper mineralization crops out near the village of Sarmeshk, Surakhe Mar, Sin Abad and Daralu (Geological Survey of Iran 1972).

The study area is located in a semi-arid environment with low vegetation, so it is a suitable test site for remote sensing studies.

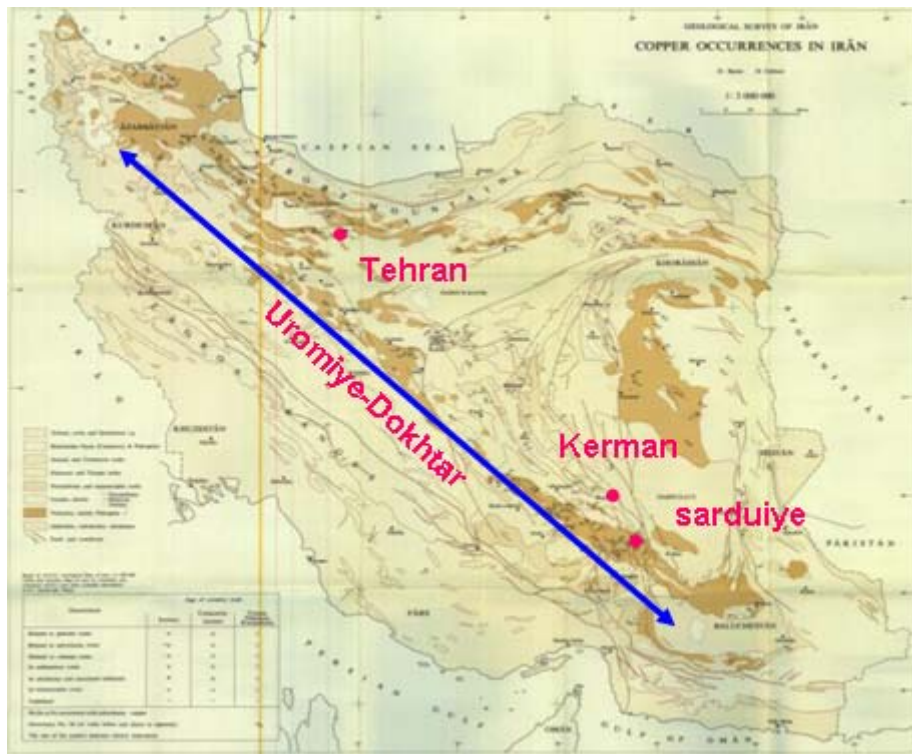


Fig.1. Location of the study area

3- ASTER Data:

The Advanced Spaceborne Thermal Emission and Reflection Radiometer (ASTER), is an advanced multispectral imager that was launched on board NASA's Terra spacecraft in December, 1999. ASTER is a cooperative effort between NASA and Japan. It records solar radiation in 14 spectral bands. This instrument providing enhanced capabilities for mineral exploration, measures reflected radiation in three bands between 0.52-0.86 μm (VNIR) and in six bands from 1.6 to 2.43 μm (SWIR), with 15 and 30 m resolution, respectively. In addition, emitted radiations are measured at 90-m resolution in five bands in the 8.125–11.65 μm wavelength regions (TIR) (Yamaguchi et al.1998, ASTER User guide 2001).

The ASTER data used in this study are level 1B data acquired on Jan 01, 2005. The images have been pre-georeferenced to UTM zone 40 North projection with WGS 84 datum. The VNIR and SWIR data were then resampled so that all 9 bands have the same 15 \times 15 m pixel size. A subset corresponding to the study area with 3183 \times 3388 pixels was derived for analytical procedures.

4- Data analysis:

The VNIR- SWIR regions of L1B dataset were radiometrically normalized using the Internal Average Relative Reflection (IARR). Spectral Angle Mapping and Linear Spectral Unmixing algorithms were implemented on the normalized data using spectra derived from the imagery and the spectra of alteration minerals selected from library of the U.S Geological Survey (USGS).

Since the kaolinite, muscovite and montmorillonite show absorption features in band 6 (centered 2.2050 μm) of ASTER they can not be discriminated from each other, so

are considered as one group. The spectra of advanced argillic minerals (alunite and pyrophyllite) are characterized by a diagnostic absorption feature in band 5 (centered 1.165 μm) of ASTER. Calcite, chlorite and epidote also were considered as one group (propylitic alteration group) because of their absorption feature in band 8 (centered 2.330 μm). Therefore we used the spectra of kaolinite, alunite and chlorite to discriminate the alteration zones.

4-1- Endmember selection:

Spectra of the image could extract from the "spectral end-member selection" procedure, including minimum noise fraction (MNF), pixel purity index (PPI) and n-dimensional visualization.

4-1-1- Minimum noise fraction transformation:

The minimum noise fraction (MNF) transformation is used to determine the inherent dimensionality of image data, to segregate noise in the data, and to reduce the computational requirements for subsequent processing (Boardman and Kruse, 1994). The inherent dimensionality of the data is determined by examination of the eigenvalues and associated eigenimages. The data space is divided into two parts: one associated with large eigenvalues and coherent eigenimages, and a second with near-unity eigenvalues and noise-dominated images. By using only the coherent portions in subsequent processing, the noise is separated from the data, thus improving spectral processing results. In a common practice, MNF components with eigenvalues less than 1 are usually excluded from the data as noise in order to improve the subsequent spectral processing results (Qui et al. 2006).

The MNF procedure was applied on the IARR data, since the eigenvalues of all MNF eigenimages of the data were greater than 1, so all the 9 bands were retained for subsequent data processing.

4-1-2- Pixel purity index:

The Pixel purity index (PPI) is a means to determine automatically the relative purity of the pixels from the higher order MNF eigenimages (Boardman, 1993; Boardman et al., 1995). The Pixel Purity Index is computed by repeatedly projecting n -dimensional scatter plots onto a random unit vector. The extreme pixels in each projection are recorded and the total number of times each pixel is marked as extreme is noted. A 'pixel purity image' is created in which the digital number (DN) of each pixel corresponds to the number of times that pixel was recorded as extreme.

Pixel Purity Index was implemented on the MNF images. To select the most pure pixels a 10000 projection of the scatter plot and the threshold factor of 2.5 were applied on the data. Density slice thresholds were used to determine pixels with high DN or pure pixels. These values were applied to computing the region of interest (ROI), being used for n-dimensional visualization.

4-1-3- n-Dimensional endmember visualization:

N- Dimensional Visualization used in conjunction with the MNF and PPI results in locating, identifying, and clustering the purest pixels and most extreme spectral responses in a data set.

N-Dimensional visualization was applied on the MNF images to extract pure pixels. After pure pixels were found the spectra of them were determined. Five major types of endmembers were extracted. These spectra could be derived from IARR images based on the spatial locations or can be taken from MNF images by inverting the

endmember) present within the pixel. Sub-pixel analysis methods can be used to calculate the quantity of target materials in each pixel of an image. The results of spectral unmixing appear as a series of gray-scale images, one for each endmember, plus a root-mean-square (RMS) error image. Higher abundances (and higher errors for the RMS error image) are represented by brighter pixels. The unmixing results should have a data range (representing endmember abundance) from 0-1. However, negative values and values greater than one are possible (Van Deer Meer 1995, 1996, 1999, 2001).

Spectral unmixing results are highly dependent on the input endmembers and changing the endmembers changes the results. A major problem in a spectral unmixing is the selection of the endmember that best represent the spectral dimensionality and spectral variability of the image data. The RMA error image can be used to select additional endmember or to repositioning endmember in subsequent analysis. To produce values lower than one an iterative procedure proposed to reach to an optimum spectral characterization of the image data through optimization criteria applied to the RMS error estimates assuming the use of derived image endmembers (Van Deer Meer 1999).

Linear Spectral Unmixing algorithm implemented on the ASTER IARR dataset and due to abundances greater than one it iterate for 4 times to reach abundances lower than one. This was performed by investigating RMS error and gray scale images and determining the area which has high error. Since in this method all of the endmembers must be chosen, all endmembers of the image were selected.

The discriminated area was similar to the area determined by SAM algorithm, corresponds to the alteration zones around copper deposits. However, the numbers of pixels known as alunite are lower in LSU images (Figure 3). This method is also useful for determining the abundance of each matter in the pixel.

Implementing LSU by the use of USGS spectra couldn't discriminate the interested areas. This may be due to the wrong selection of the endmembers, because this algorithm is highly dependent on the input endmembers, and changing the endmembers changes the results.

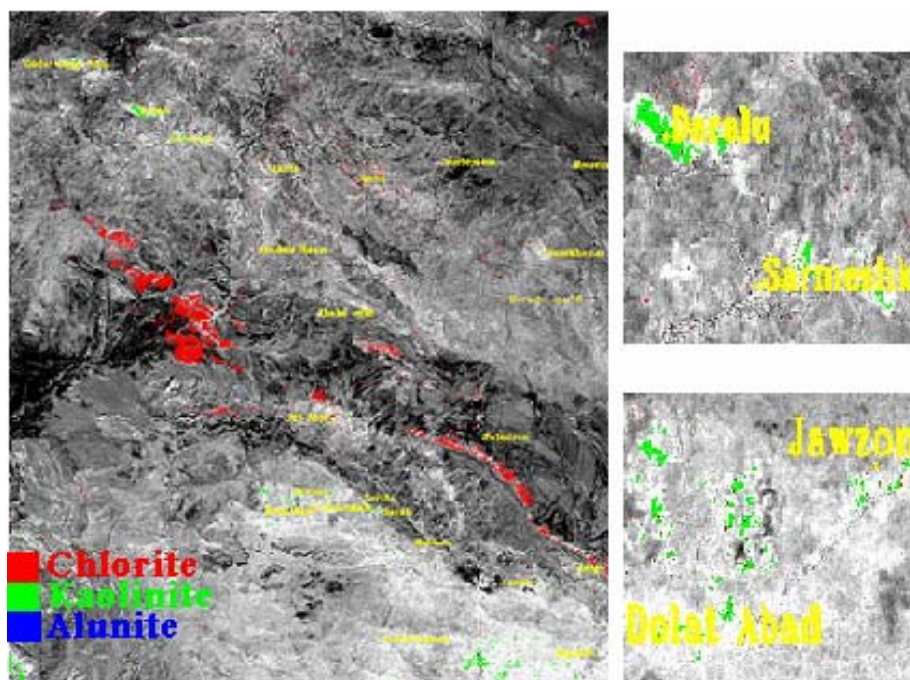


Fig 3- Areas discriminate with Linear Spectral Unmixing using image spectra

5- Summary and conclusion:

This paper has investigated the SAM and LSU algorithms for mapping alteration zones using ASTER data. ASTER data provide not only improved spatial and radiometric resolutions, but also much more spectral information when compared to the traditional multi spectral remote sensing data such as Landsat TM/ETM⁺.

SAM and LSU were implemented based on the comparison of pixel spectrum with the spectra of known pure materials or endmembers. The endmembers were supplied from the USGS spectral library and the image spectra in this study. The image spectra were extracted from the "spectral end-member selection" procedures, including minimum noise fraction (MNF), pixel purity index (PPI) and n-dimensional visualization.

Implementing Spectral Angle Mapping with the image spectra and the USGS resampled spectra represent similar areas corresponding to the alteration zones around copper deposits. Spectra derived from the ASTER imagery are more reliable than the library spectra.

Iterative Linear Spectral Unmixing using image spectra obtained reasonable results and successfully discriminated pixels with highest proportions of alteration minerals, while the output abundance values for endmembers selected from the USGS spectral library were not satisfied.

Acknowledgment:

We would like to thank the Research Council of Shiraz University for providing the necessary funds and The Australian Geological and Remote Sensing Services (AGARSS) for spectral analyze of Field spectra

References:

- Boardman, J.W., 1993. Automating spectral unmixing of AVIRIS data using convex geometry concepts. In: Summaries of the 4th Annual JPL Air-borne Geoscience Workshop, Pasadena, pp. 11–14.
- Boardman, J.W. and Kruse, F.A., 1994. Automated spectral analysis: a geologic example using AVIRIS data, North Grapevine Mountains, Nevada. In Proceedings of the Tenth Thematic Conference on Geologic Remote Sensing, 9–12 May, San Antonio, Texas (Ann Arbor, MI: Environmental Research Institute of Michigan), P. 407–418.
- Boardman, J.W., Kruse, F. A., and Green, R. O., 1995. Mapping target signatures via partial unmixing of AVIRIS data: in Summaries, Fifth JPL Airborne Earth Science Workshop, JPL Publication 95-1, v. 1, p. 23-26.
- ENVI User's Guide, 2003 "ENVI User's Guide V. 4.0" Research Systems, Inc, P.1084.
- Galvao L.S, Filho R.A, Vitorello.C, 2001. Spectral discrimination of hydrothermal altered materials using ASTER Short – wave infrared bands: Evaluation in a tropical Savannah Environment. International Journal of Applied Earht Observation and Geoinformation, V.7, P. 107-114.
- Geological Survey of Iran, Geological map of Sarduiye 1:100000 SHEET 7447, 1972
- Geological Survey of Iran, 1973, Exploration for Ore Deposits in Kerman Region. Report No,Yu/53
- Kruse. F. A., Lefkoff, A. B., Boardman, J. B., Heidebrecht, K. B., Shapiro, A. T., Barloon, P. J., and Goetz, A. F. H. 1993. The Spectral Image Processing System

- (SIPS) - Interactive Visualization and Analysis of Imaging spectrometer Data. Remote Sensing of Environment. V. 44, p. 145 – 163
- .Qiu, F. Abdelsalam, M. Thakka, P. 2006, Spectral analysis of ASTER data covering part of the Neoproterozoic Allaqi-Heiani suture, Southern Egypt. Journal of African Earth Sciences., Vol. 44, pp.169–180.
- Rown. L.C,Hook.S.J, Abrams.M.J,Mars.J.C, 2003, Mapping hydrothermally altered rocks at Cuprite, Nevada, using the Advanced Spaceborne Thermal Emission and Reflection Radiometer (ASTER) a new satellite imaging system" V.95, P.1019-1027
- Rown.L.C, Schmidt .R.G,Mars.J.C, 2006, Distribution of hydrothermally altered rocks in Reko Diq ,Pakistan mineralized area based on spectra analysis of ASTER data "Remote Sensing of Environment V.104, P.74-87
- Tangestani.M .H , Mazhari.N ,Agar.B, 2005, Mapping the porphyry copper alteration zones at the Meiduk areas , SE Iran, using the Advanced Spaceborne Thermal Emission and Reflection Radiometer (ASTER) data" SPIE, V.59830.59830,S P.1-10
- Tangestani M.H, Mazhari M, Agar, Moore F. 2008, Evaluating Advanced Spaceborne Thermal Emission and Reflection Radiometer (ASTER) data for alteration zone enhancement in a semiarid area, northern Shahr-e-Babak, SE Iran. International Journal of Remote Sensing. V. 29, No. 10, P. 2833–2850
- Yamaguchi.Y, Khale.A.B, Tsu.H, Kawakami.T, Pniel.M, 1998, Overview of Advanced Spaceborne Thermal Emission and Reflection Radiometer (ASTER. IEEE Transaction on Geoscience and Remote Sensing. V. 36, P.1062- 1071.
- Van Der Meer.F 1995, Spectral unmixing of Landsat Thematic Mapper data. INT.J.Remote Sensing, V. 16NO.16, P.3189-319
- Van Der Meer.F, 1996, Spectral mixture modeling and spectral stratigraphy in carbonate lithofacies mapping. ISPRS Journal of Photogrammetry & Remote Sensing v.51, P.150-162
- Van Der Meer.F, 1999, Iterative Spectral Unmixing. INT.J.Remote Sensing, V.20, NO.17 P.3431-3436
- Van Der Meer.F, Dejong S.M, 2001, Remote sensing and digital image processing. imaging spectroscopy Kluwer Academic publited in the Netherlands V.4, 306P